Wind-Forced Variability of Upper Ocean Dynamics in the Central Equatorial Pacific during PEQUOD[1]

ARTHUR VOORHIS, JAMES R. LUYTEN, GERALD NEEDELL AND JOHN THOMSON

Woods Hole Oceanographic Institution, Woods Hole, MA 02543

(Manuscript received 11 March 1983, in final form 8 November 1983)

ABSTRACT

Horizontal currents and dynamic height anomalies measured with a vertical profiler in the central equatorial Pacific during January 1981, February 1982 and April 1982 show significant changes in the upper ocean which are analyzed and discussed in terms of the vertical baroclinic modal structure. Most noticeable was a marked increase in average undercurrent speed and transport from February to April 1982, which was accompanied by a raising of sea level and a deepening of the pycnocline. This was due to an average increase in both first and second baroclinic modes. Over half of the increase of the first mode was due to a Kelvin wave pulse propagating eastward through the survey area at an estimated speed of 300 cm s^{-1}. Evidence is presented which indicates that the wave was forced by a tropical storm in the western Pacific. The increase in the second baroclinic mode is attributed to the large-scale relaxation of the trade winds in the central and western Pacific during the spring of 1982.

1. Introduction

Meteorological studies and global numerical models suggest that there is a special sensitivity of global climate to changes in sea-surface and near-surface conditions in the oceanic equatorial zone. In order to predict these changes it is necessary to understand the dynamic response of the equatorial ocean to large-scale atmospheric forcing. This response depends not only on local forcing, but also on the advection resulting primarily from the baroclinic response to remote forcing. Outside of the equatorial zone, the mechanism for the latter response is understood to be slow, although complex, geostrophic adjustment to Ekman pumping on the time scale of years. Within the zone, however, dynamic models suggest that the remote response to large-scale forcing is more rapid and is determined by the zonal transit times of equatorially trapped, internal Kelvin and Rossby waves generated at the boundaries and by convergence and divergence of the directly forced near-surface current. The trans-Pacific travel times for the gravest-mode Kelvin (eastward) and Rossby (westward) waves are of the order of 60 and 180 days respectively. Wyrtki (1975) has suggested, in fact, that anomalous surface conditions in the western Pacific propagated eastward as a Kelvin wave and triggered or influenced catastrophic events, such as El Niño, along the eastern boundary off Peru.

In the following, we present new data from the central equatorial Pacific obtained during the Pacific Equatorial Dynamics Program (PEQUOD) in 1981 and 1982 using a high-resolution vertical profiler from surface to bottom. In Section 2, we describe briefly the field program, instrumentation and data analysis. In Section 3, we present the results and describe the differences found both in the upper 500 meters and in the vertical baroclinic modal structure of the entire water column. In Section 4, we present evidence that these differences were due primarily to the eastward propagation of disturbances through the survey area. From comparisons with historical and recent data and with predictions from numerical models, we argue in Section 5 that the observed variability is largely due to changes in wind stress forcing primarily in the western equatorial Pacific on seasonal and on short, event-like, time scales.

2. Field program, instrumentation and analysis

The data reported here were collected on three cruises, each approximately a month in duration, to the central equatorial Pacific aboard the R.V. *Thomas G. Thompson* in January 1981, February 1982 and April 1982. On each cruise vertical profiles of horizontal current, pressure, temperature and conductivity (salinity) were measured from surface to bottom (4200 to 4600 m) at 17 sites, A–Q shown in Fig. 1, between 138 and 153°W. Site sampling always began in the east and ended in the west, but differed in detail from cruise to cruise, primarily because of repeated sampling

[1] PEQUOD Contribution No. 19 and Woods Hole Oceanographic Institution Contribution No. 5352.

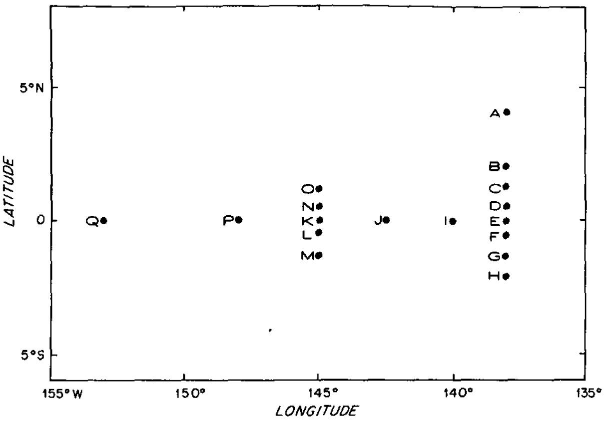

FIG. 1. Position of dropsonde sites occupied on each cruise.

along 145°W longitude. For example, the zonal–temporal sampling scheme in April 1982 is shown in Fig. 2.

The instrument used to obtain the data was a free-fall acoustic dropsonde (the White Horse), also employed by Luyten and Swallow (1976) and Eriksen (1981) in the discovery of deep equatorial jets in the Indian and Pacific Oceans. In order to track the dropsonde, three transponders were deployed on the ocean floor, surveyed at each site during the first cruise and were left on the bottom and used again when the sites were reoccupied on the later two cruises. Usually, only one deployment of the dropsonde was made when occupying a site. This provided two vertical profiles of data: one during the instrument's descent and the other during its ascent. The time between launch and recovery (typically about three hours) was usually used to occupy a hydrographic station for calibration of the conductivity cell of the CTD in the dropsonde.

The performance and calibration of the dropsonde has been described by Luyten *et al.* (1982). Its descent (and ascent) rate was approximately one meter per second. Currents were determined by tracking its position relative to the transponders every 15 s (15 m vertical intervals) with a horizontal accuracy of about 1 m. Because it essentially measures transport, averaging over larger vertical intervals Δz reduces random errors in computed horizontal velocity Δv, according to the uncertainty relation, $\Delta z \Delta v \approx 1 \times 10^4$ cm^2 s^{-1}. Temperature, salinity (conductivity) and pressure were sampled every second (1 m vertical intervals) during descent and ascent with random uncertainties of 0.003°C, 0.005‰ and 2 db. The long-term drift of salinity measurements from site to site was less than 0.005‰.

Prior to analysis, all dropsonde data were edited and smoothed to give, for each site, profiles of zonal and meridional velocity interpolated at 25 m depth intervals and profiles of temperature, salinity, computed density and computed dynamic height anomaly interpolated at 2 m depth intervals.

The final site profiles of velocity components, U positive eastward and V positive northward, and dynamic height anomaly D relative to 4100 db were then decomposed formally into the usual vertical dynamical modes (Taylor, 1936; Gill and Clarke, 1974) appro-

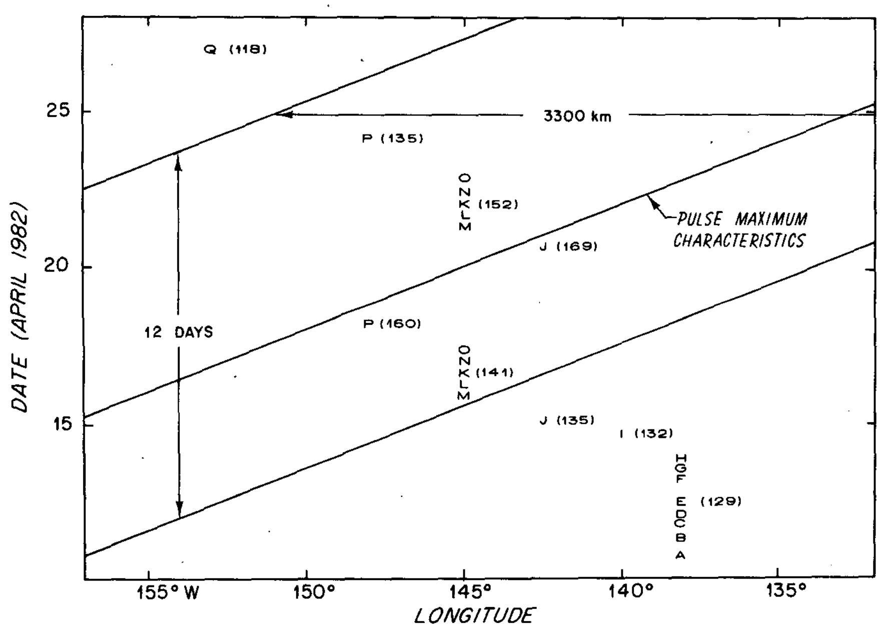

FIG. 2. Zonal site sampling as a function of time in April 1982. Shown in parentheses alongside each equatorial site is the measured undercurrent maximum speed in cm s^{-1}. Also shown are propagation characteristics for the Kelvin wave pulse described in text.

priate to the stratification measured in the survey area. That is, we computed the modal amplitudes given by

$$\begin{Bmatrix} U_n \\ V_n \\ D_n \end{Bmatrix} = \frac{1}{H}\int_{-H}^{0} dz F_n(z) \begin{Bmatrix} U \\ V \\ D \end{Bmatrix}, \tag{1}$$

where z is positive upwards, H the water depth (4100 m) and F_n is the appropriate eigenfunction for the nth bottom trapped mode in a 4100 m deep ocean at rest. The F_n are dimensionless and orthonormal, i.e.,

$$\frac{1}{H}\int_{-H}^{0} dz F_n(z)F_m(z) = \begin{cases} 1, & n = m \\ 0, & n \neq m, \end{cases} \tag{2}$$

and are determined from

$$F_n(z) = \frac{C_n}{\bar{N}}\frac{dG_n}{dz}, \tag{3}$$

where

$$\frac{d^2G_n}{dz^2} + \frac{N^2(z)}{C_n^2}G_n = 0 \tag{4}$$

with the boundary condition $G_n = 0$ at $z = 0, -4100$ m. In the above, C_n is an eigenspeed (equal to the phase speed of the nth bottom trapped Kelvin wave) and $\bar{N}$ is the depth-average value of the Brunt-Väisälä frequency profile $N(z)$. The profile used to compute the eigenfunctions is shown in Fig. 3 along with the resulting eigenfunctions F_1, F_2 of the two gravest baroclinic modes.

Dynamic height is defined and computed in such a way that the modal amplitudes D_n from Eq. (1) are composed of two parts: a large constant part of no interest and a small varying part which is of dynamic

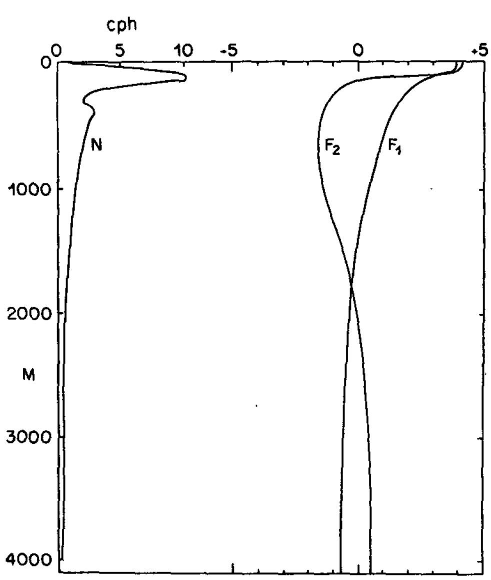

FIG. 3. Vertical profiles of Brunt-Väisälä frequency (left) and of the gravest two baroclinic horizontal eigenmodes (right) in the central equatorial Pacific.

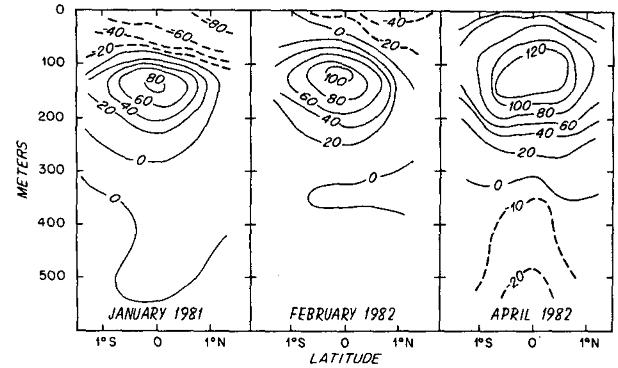

FIG. 4. Meridional and vertical structure of the zonal current (cm s^{-1}) in the upper ocean averaged over longitude and time for each cruise period. Solid contours represent eastward flow.

interest. We were only concerned with the latter. In addition, the amplitude of the barotropic mode D_0 of dynamic height could not be computed because absolute pressure measurements were not available.

The uncertainty in the calculated modal amplitudes of current (U_n, V_n) due to tracking errors is estimated to be less than 0.4 cm s^{-1}. The uncertainty in the modal amplitudes D_n of dynamic height anomaly relative to 4100 db is estimated to be less than 0.2 dynamic centimeters.

3. Results

a. Local wind stress

The average local wind stress over the survey area between 2°N and 2°S latitudes was computed for each cruise period using the relation $\rho_a C_d |V| \mathbf{V}$ where $\rho_a = 1.2 \times 10^{-3}$ gm cm^{-3}, $C_d = 1.5 \times 10^{-3}$ and $\mathbf{V}$ is the vector wind velocity measured from hourly shipboard observations of relative wind speed and direction corrected for ship speed and heading. The daily prevailing wind was westward on all cruises. The average westward zonal component of stress was largest (-0.77 ± 0.14 dyn cm^{-2}) in January 1981; next largest (-0.70 ± 0.23 dyn cm^{-2}) in February 1982; and smallest (-0.45 ± 0.14 dyn cm^{-2}) in April 1982. The average meridional component of stress was always less than 10% of the above values.

b. Upper ocean

The mean zonal component of current in the upper ocean (above 500 m) in each cruise period differed markedly in intensity and in vertical and meridional structure. This is illustrated in Fig. 4 where the current contours are averages over a maximum time scale of 20 days and a maximum zonal scale of 1650 km (Fig. 1). Above 300 m the eastward undercurrent was rather weakly developed in January 1981, and was overlain by strong westward flow. In February 1982 the undercurrent was stronger and the westward surface flow weaker. In April 1982 the undercurrent was very intense and had "surfaced" with eastward surface current flowing upwind. Over the two months separating the latter cruises, the mean undercurrent maximum speed increased by a factor of 1.3 while the mean eastward transport in the upper 300 m between 2°N and 2°S latitudes increased by a factor of 2.4 from 26 to 62 ($\times 10^6$ m^3 s^{-1}) (26–62 Sv). The difference in these two ratios reflects the fact that the eastward zonal current in the upper 300 m increased not only in intensity but also in meridional scale. Below 300 m the situation was quite different. The zonal current was weak and variable in January 1981; weak and predominantly eastward in February 1982; and westward in April 1982.

The above was accompanied by marked changes in upper ocean baroclinicity. Shown in Fig. 5 is the zonal variation along the equator of surface dynamic height anomaly relative to 4100 db for the three cruise periods. The sea surface, although showing considerable small-scale structure, sloped upwards to the west relative to the 4100 db surface in each period. As a result, the pressure gradient of the surface was always opposed to the prevailing local wind stress which was westward on each cruise. More significant, however, is the average increase of approximately 10 cm in surface height during April 1982 versus that in either February 1982 or January 1981, the last two records being quite similar. Of this increase, about 90 percent was due to a 25 m deepening of the upper ocean pycnocline (average depth 120 m) and 10 percent due to a 2°C warming of surface water in April.

c. *Modal variability*

The equatorial variance of the amplitudes U_n, V_n, D_n [Eq. (1)] of the first ten modes is shown in Fig. 6 for three "time" scales. The "total" variance is from the mean amplitude over all equatorial sites (E, I, J, K, P, Q) from *all* cruises which spans a time scale of 16 months and a zonal scale of 1600 km. The "cruise" variance is the average variance from the mean of *each* cruise over the same sites and spans a time scale of 20 days and zonal scale of 1600 km. The "24-hour" variance is from the mean of seven measurements carried out over a 24-hour period at Site Q during April 1982.

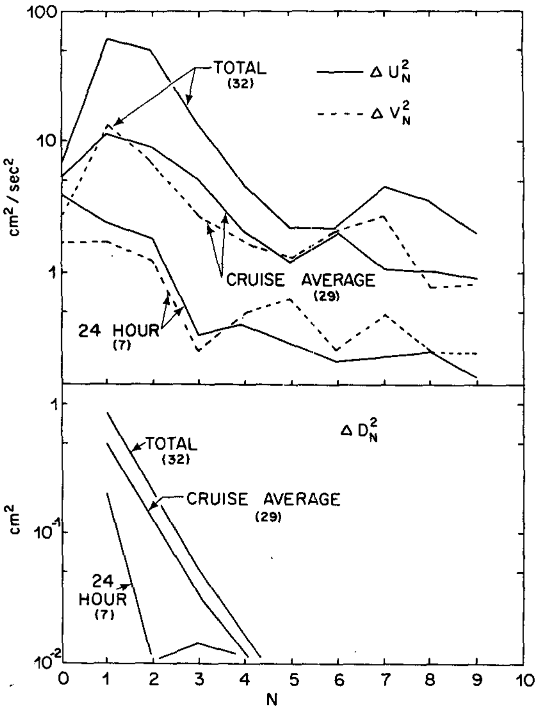

FIG. 6. Variance at the equator of the first ten modal amplitudes of zonal and meridional velocity (upper) and dynamic height anomaly (lower) relative to 4100 db for three sampling ranges (see text).

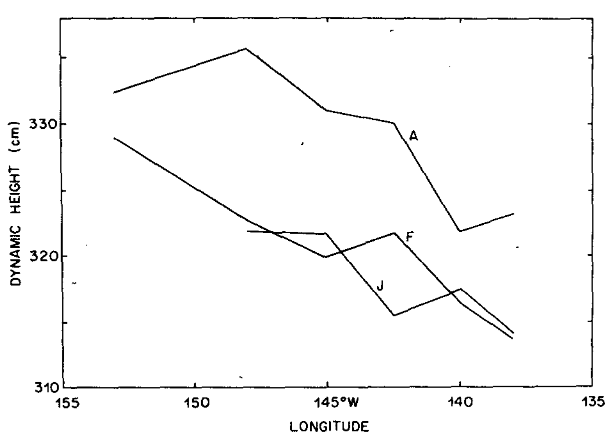

FIG. 5. Zonal variation along the equator of the surface dynamic height anomaly relative to 4100 db for each cruise period (J—January 1981, F—February 1982, A—April 1982).

Baroclinic ($n \geq 1$) current variance clearly exceeds barotropic ($n = 0$) variance for the two longest time scales. At all time scales, the baroclinic variance is dominated by the first two modes ($n = 1, 2$) for both current and pressure, particularly the latter, whose modal distribution is "redder" than the former. In fact, the variance of D_n beyond mode four could not be computed because it was less than that due to measurement (salinity) noise.

Comparing the variance of pressure and current over the three time scales suggests that frequency spectra for the gravest baroclinic modes is redder for U_n than for either V_n or D_n. In fact, the total variance of U_n is due primarily to intercruise changes, while for V_n, it is not and is practically the same as that observed during each cruise. The intercruise variations of the average U_n over all equatorial sites were particularly interesting and are shown for the first ten modes in Fig. 7. Referring to Fig. 4, one sees that the changing vertical structure in the upper 500 m is due primarily to increases in the first two baroclinic modes. In par-

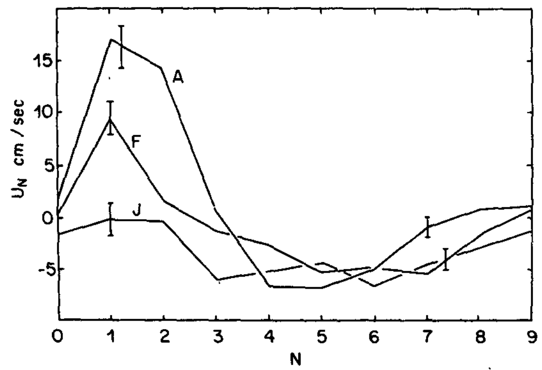

FIG. 7. Average amplitude over all equatorial sites of the first ten modes of zonal velocity for each cruise period (J—January 1981, F—February 1982, A—April 1982).

ticular, the occurrence of a marked westward current below 300 m in April 1982 was due to an increase in the second baroclinic mode which has a shallow current node (Fig. 3) at 160 m.

The preceding concerns modal variations on the equator. Meridional variations were more difficult to analyze because of the rather poor meridional resolution (Fig. 1) and the relatively low number of sites sampled (only one site sampling at Lats. 2°N and 2°S per cruise). Shown in Figs. 8 and 9 are the mean am-

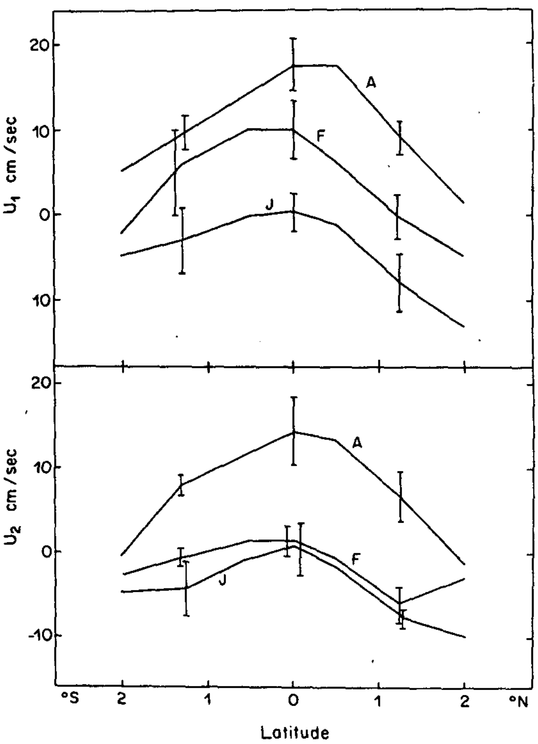

FIG. 8. Average meridional variation, from 138 and 145°W longitude, of the amplitudes of the first (upper) and second (lower) baroclinic modes of zonal velocity for each cruise period. (J—January 1981, F—February 1982, A—April 1982).

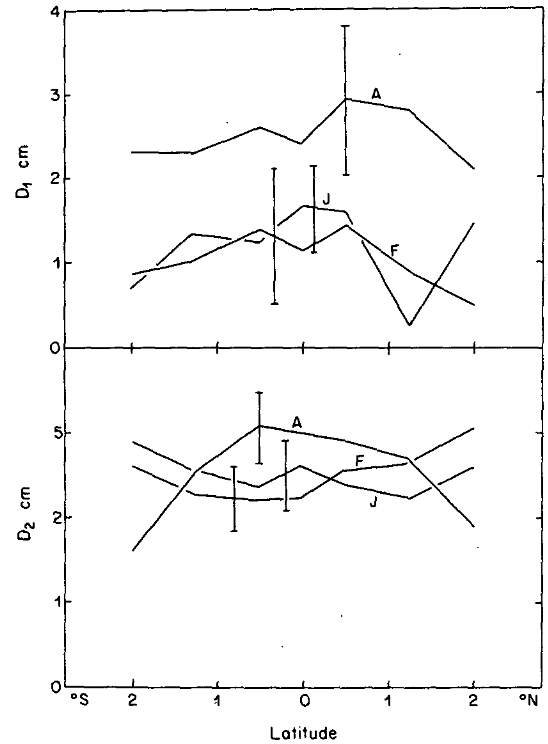

FIG. 9. As in Fig. 8 but of dynamic height anomaly relative to 4100 db.

plitudes of U_1, U_2 and D_1, D_2 as a function of latitude for each cruise period. They were determined by combining measurements from sites along 138 and 145°W and represent averages over periods of 15 days and zonal scales of 700 km.

In general, the meridional structures of U_n and D_n differ. Whereas the former have maximum amplitudes at or near the equator and decrease rapidly to the north and south, the latter do not and are dominated by larger meridional scales. This is not, perhaps, surprising if the meridional momentum balance is primarily geostrophic, which requires the zonal current to be balanced by the meridional gradient of dynamic height. Unfortunately, such a geostrophic balance could not be tested here because of the poor resolution and sampling and because of the relatively large variation of dynamic height on the cruise time scale (Fig. 6, lower panel). What is most significant, however, is the *change* in meridional structure from cruise to cruise, particularly from February to April 1982. The increase of U_1 and D_1 was over a larger meridional scale (greater than 200 km) than could be resolved. The same was true for U_2 and D_2, although the data suggest that the increase was over a somewhat small meridional scale.

4. Equatorial waves

One reason for the intensification of the undercurrent in April 1982 can be detected in the temporal–

zonal sampling diagram (Fig. 2) for the cruise. The maximum eastward undercurrent is shown in parentheses alongside each equatorial site and an examination of those numbers suggests that a current pulse was encountered with maximum eastward flow occurring near 145°W sometime between 18 and 22 April. Since it appears that our sampling traversed the pulse only once, its structure, although distorted in space and time, should be resolved unambiguously in the equatorial data by plotting it sequentially as a simple time series starting in the east and ending in the west. The modal amplitudes U_1, D_1, U_2, D_2 at the equator are shown in such a series in Fig. 10 for the April cruise and for the previous cruise, two months earlier in February. The values of D_1 and D_2 give the deviations from the mean at 145°W (Site K) in February. Furthermore, they have been corrected for the presence of a mean zonal gradient which, in effect, removed an apparent time trend due to east-to-west sampling. This assumed gradient in D_1 and D_2 was just that required to balance the measured mean local zonal component of the wind stress τ and was computed to a good approximation, using the notation of Eq. (1), from the relation $\tau F_n(0)/\rho H$ where $n = 1, 2$ and ρ is the water density (1 g cm^{-3}).

The pulse detected in the April data appears in Fig. 10 to be due to the first vertical baroclinic mode only

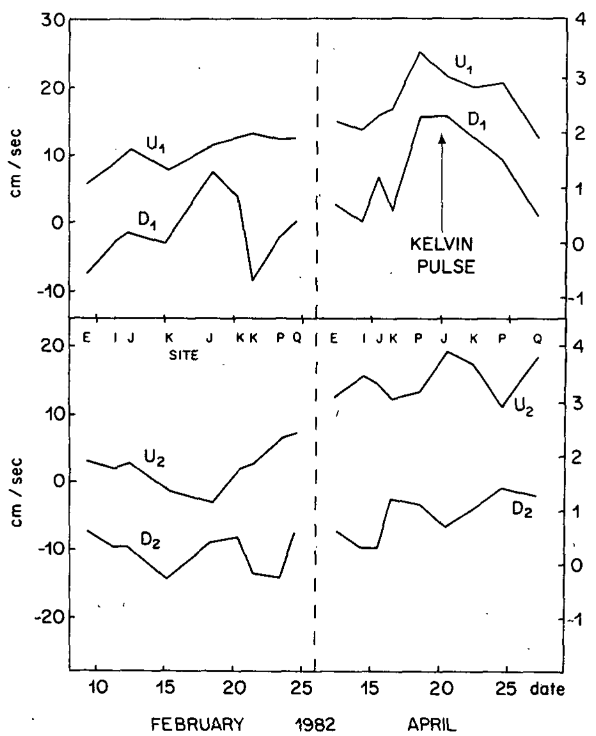

FIG. 10. Time series of the amplitudes on the equator of the first (upper) and second (lower) baroclinic modes of zonal velocity and of dynamic height anomaly relative to 4100 db for the February and April 1982 cruises.

and it contributes more than half of the average increase from February to April for this mode (Fig. 7). The fluctuations, ΔD_1 and ΔU_1, associated with the pulse are highly correlated (+0.92), are in phase and have an apparently large meridional scale (Figs. 8 and 9) exceeding 200 km. The ratio $\Delta D_1/\Delta U_1$, from linear regression, lies between 110 and 240 cm s^{-1} within 95% confidence limits. These properties are reasonably consistent with those of a gravest baroclinic mode, bottom-trapped Kelvin wave-pulse propagating eastward through the survey area. For such a pulse in a still ocean 4100 m deep, one finds the eigensolution of Eq. (4) a meridional amplitude scale (*e*-folding) of 480 km and a fluctuation ratio $\Delta D_1/\Delta U_1 = C_1 = +270$ cm s^{-1}, where C_1 is its eastward phase speed. A first-order correction[2] for the Doppler shift by a mean zonal current, taken to be the average found in February (Fig. 4), alters the above slightly to $\Delta D_1/\Delta U_1 \approx 230$ cm s^{-1}, $C_1 \approx 300$ cm s^{-1}. Assuming the above corrected phase speed, one infers that the pulse maximum, and its leading and trailing edges, propagated along the characteristics shown in Fig. 2, which implies that the time and space scales are approximately 12 days and 3300 km, as indicated.

Aside from the above, it was not possible to correlate with reasonable certainty[3] other variations of pressure and zonal velocity in Fig. 10, or of meridional velocity (not shown), with any of the broad spectrum of available equatorially trapped motions. The marked increase in the average zonal velocity $\Delta\bar{U}_2$ of the second mode and lesser increase in average pressure $\Delta\bar{D}_2$ from February to April does not appear to be due to a short-term pulse but, rather, has a time scale of a month or longer. This and the change in meridional structure of the second mode (Figs. 8 and 9) suggest some kind of large-scale Kelvin-like disturbance. The ratio $\Delta\bar{D}_2/\Delta\bar{U}_2$, however, is of the order of +50 cm s^{-1} which is considerably less than that (130 cm s^{-1}) estimated for a Doppler-shifted second baroclinic Kelvin wave, indicating that the change over the two months was not due to a simple step pulse that propagated through the area between the two cruises. If one interprets the linear time trend of D_2, shown for April in Fig. 10, as due solely to westward sampling in the presence of a mean zonal gradient, one can estimate the latter to be of the order of 6×10^{-4} dyn cm km^{-1}. This gradient is unbalanced by the local wind stress (the effect of the latter having been removed, as described previously) and is in such a direction as to

[2] A first-order correction is a first-order perturbation expansion in the Rossby number U/C_1, where U is the maximum amplitude of the mean zonal undercurrent (McPhaden and Knox, 1979).

[3] The small out-of-phase fluctuations of U_2 and D_2 during April in Fig. 10 were particularly interesting. We suggest they are due to sampling westward and eastward (Fig. 2) across a nearly stationary or slowly westward moving disturbance with a zonal wavelength of 1300–1400 km.

accelerate the zonal current associated with the second mode eastward by 15 cm s^{-1} over a period of one month. This is more than enough to explain the average increase observed and suggests that the second mode was still intensifying during the April cruise.

5. Discussion

Long-term sea level records from island tide stations show that the baroclinic response of the equatorial Pacific to wind forcing, although complex, can be characterized (Wyrtki, 1983), roughly, as consisting of two parts: a slowly changing background level over periods of months or longer due to large-scale periodic (seasonal, etc.) and an aperiodic forcing, on which are superimposed numerous pulses having a duration of one to three weeks. The latter, first documented by Knox and Halpern (1982), are due to Kelvin wave pulses generated primarily by short-term westerly wind events in the western Pacific primarily during the spring months, which propagate eastward along the equatorial wave guide at a speed of approximately 300 cm s^{-1}.

The gravest baroclinic-mode Kelvin pulse resolved in our April 1982 data is undoubtedly one of the above pulses and, subsequently, has been identified by others (Wyrtki, 1983; Lucas, private communication, 1983; Hayes, 1983) in island sea level records on its transit eastward across the Pacific. Maximum pulse levels, from west to east, were observed at Nauru (1°S, 167°E) on approximately 1 April; Jarvis (0°, 160°W) on 15 April; Christmas (2°N, 157°W) on 15 April; Isabela (1°S, 91°W) on 15 May; and Santa Cruz (1°S, 91°W) on 15 May. Tropical weather surface pressure charts (U.S. Department of Commerce, NOAA, 1982) show that the forcing event for this pulse most consistent with its subsequent history was the tropical cyclone pair, Bernie—Odessa. Straddling the equator between 150 and 165°E, this pair intensified over a period of several days at the end of March, generating eastward winds at the equator in excess of 30 knots. Subsequently, the pair separated, each migrating away from the equator, so that their influence along the equator lasted about one week. The size and duration of this event is quite consistent with the observed Kelvin pulse. The duration of such a pulse (which to first order is nondispersive) from an idealized storm is approximately $T + L/c$, where T and L are the duration and zonal scale of the storm and $c = 300$ cm s^{-1} is the pulse phase speed. The rise (and decay) time for the pulse is the smaller of T or L/c. For the pulse reported here of 12 days duration (Fig. 2), we estimate that $T \approx L/c \approx 6$ days and $L \approx 1500$ km.

Because of the spatial and temporal limits of our observations, we can only speculate about the influence of large-scale wind forcing on our data. Particularly interesting, however, is the intensification of the second baroclinic mode from February to April 1982. A similar intensification can be seen in the vertical profiles of zonal current reported by Firing and Lucas (1983) for an area on the equator farther to the west (159°W) during the same period. We suggest that this was due to the large-scale relaxation of the southeasterly trades during the spring of 1982.

Ship wind reports (Rebert *et al.*, 1983) and monthly variations of the 850 mb trade-wind anomaly index (Climate Analysis Center, NOAA, 1983) show that prevailing winds were maximum easterly (and somewhat stronger than usual) in the western Pacific during November–December 1981, and declined thereafter through June 1982, when they reversed and strengthened, signaling the collapse of the trade winds and the onset of the 1982–83 equatorial Pacific "warm event" (Halpern, 1983). In the central Pacific, the easterly trades were maximum one to two months later, in December–January, and then declined all spring and summer, becoming anomalously weak and variable by the fall of 1982. Such a relaxation in wind stress is not in equilibrium with zonal surface pressure gradients because the baroclinic adjustment time of the equatorial Pacific is of the order of 400 days (Cane, 1979). In particular, following a maximum in westward stress, the numerical models of Philander and Pacanowski (1981) predict that the surface pressure gradient is unbalanced and accelerates the current in the surface layers eastward. They show that this is particularly effective in exciting the second baroclinic mode because it has a large amplitude confined to the surface layers (Fig. 3). Had the trade winds relaxed abruptly, the acceleration would cease upon the arrival of a second baroclinic Kelvin wave from the western boundary of the relaxation region (two months travel time from western to central Pacific). Because the wind relaxation is actually distributed over time and space, the arrival of such a wave is much less distinct so that the acceleration is less intense but lasts for a longer time.

The weakening of the easterly trades in the central Pacific during the early spring of 1982 was not markedly different from that predicted from the climatological monthly variations documented by Wyrtki and Meyers (1975), Hickey (1975) and Horel (1982). This suggests that the intensification of the second baroclinic mode in our data is seasonal. Some support for this conjecture is given by the extensive current profiling data along longitudes 150, 153 and 158°W reported by Wyrtki *et al.* (1981) which show what appears to be an annual increase in the transport of the undercurrent during the months March–April in 1979 and 1980.

Acknowledgments. We are grateful to the National Science Foundation for supporting this work under Grant OCE 79-27186 as part of the Pacific Equatorial Ocean Dynamics Program (PEQUOD). We would like to thank M. B. Blumenthal and C. C. Eriksen of the Massachusetts Institute of Technology for providing the program for computing vertical eigenvalues and eigenmodes.

REFERENCES

Cane, M. A., 1979: The response of an equatorial ocean to simple wind stress patterns: II. Numerical results. *J. Mar. Res.*, **37**, 253–299.

Climate Analysis Center, 1983: Special climate diagnostics bulletin, 15 July 1983. The 1982/83 Pacific warm episode falling sea surface temperatures in the eastern equatorial Pacific. Climate Analysis Center, NOAA, National Weather Service, Washington, DC. (Unpublished manuscript).

Eriksen, C. C., 1981: Deep currents and their interpretation as equatorial waves in the western Pacific Ocean. *J. Phys. Oceanogr.*, **11**, 48–70.

Firing, E., and R. Lucas, 1983: El Niño at the equator and 159°W. *Trop. Ocean-Atmos. Newslett.*, **21**, 9–11.

Gill, A. E., and A. J. Clarke, 1974: Wind induced upwelling, coastal currents and sea-level changes. *Deep-Sea Res.*, **21**, 325–345.

Halpern, D., Eds., 1983: 1982 Equatorial Pacific warm event. *Trop. Ocean-Atmos. Newslett.*, **16**, (Special Issue) 1–19.

Hayes, S. P., 1983: The 1982 event in the Galapagos Sea level array. *Trop. Ocean-Atmos. Newslett.*, **16**, 17–18.

Hickey, B., 1975: The relationship between fluctuations in sea level, wind stress and sea surface temperature in the equatorial Pacific. *J. Phys. Oceanogr.*, **5**, 460–475.

Horel, J. D., 1982: The annual cycle in the tropical Pacific atmosphere and ocean. *Mon. Wea. Rev.*, **110**, 1863–1878.

Knox, R. A., and D. Halpern, 1982: Long range Kelvin wave propagation of transport variations in Pacific Ocean equatorial currents. *J. Mar. Res.*, **40**(Suppl.), 329–339.

Luyten, J. R., and J. C. Swallow, 1976: Equatorial undercurrents. *Deep-Sea Res.*, **23**, 999–1001.

——, G. Needell and J. Thomson, 1982: An acoustic dropsonde—design, performance and evaluation. *Deep-Sea Res.*, **29**, 499–524.

McPhaden, M. J., and R. A. Knox, 1979: Equatorial Kelvin and inertio-gravity waves in zonal shear flow. *J. Phys. Oceanogr.*, **9**, 263–277.

Philander, S. G. H., and R. C. Pacanowski, 1981: Response of equatorial oceans to periodic forcing. *J. Geophys. Res.*, **86**, 1903–1916.

Rebert, J., J. Donguy, G. Eldin and A. Morliere, 1983: Thermal fluctuations in the equatorial Pacific in relation to the 1982–83 warm event. *Trop. Ocean-Atmosp. Newslett.*, **21**, 7–8.

Taylor, G. I., 1936: Oscillations of the atmosphere. *Proc. Roy. Soc. London*, **A156**, 318–326.

U.S. Department of Commerce, NOAA, 1982: Mercator tropical analysis, surface pressure sheets, 15 March–15 April, 1982. Environmental Data and Information Service, Asheville, NC.

Wyrtki, K., 1975: El Niño—the dynamic response of the equatorial Pacific Ocean to atmospheric forcing. *J. Phys. Oceanogr.*, **5**, 572–584.

——, 1983: Sea level in the equatorial Pacific in 1982. *Trop. Ocean-Atmos. Newslett.*, **21**, 7–8.

——, and G. Meyers, 1975: The trade wind field over the Pacific Ocean. Part II: Bimonthly fields of wind stress: 1950 to 1972. Hawaiian Inst. Geophys. Rep. HIG72-2, University of Hawaii, 16 pp.

——, E. Firing, D. Halpern, R. Knox, G. McNally, W. C. Patzert, E. D. Stroup, B. A. Taft and R. Williams, 1981: The Hawaii-to-Tahiti Shuttle Experiment. *Science*, **211**, 22–28.